AIP | Applied Physics Letters

Strain-induced energy gap variation in ZnTe/ZnMgTe core/shell nanowires

P. Wojnar, M. Zielinski, E. Janik, W. Zaleszczyk, T. Wojciechowski, R. Wojnar, M. Szymura, . Kopotowski, L. T. Baczewski, A. Pietruchik, M. Wiater, S. Kret, G. Karczewski, T. Wojtowicz, and J. Kossut

Citation: Applied Physics Letters **104**, 163111 (2014); doi: 10.1063/1.4873355
View online: http://dx.doi.org/10.1063/1.4873355
View Table of Contents: http://scitation.aip.org/content/aip/journal/apl/104/16?ver=pdfcov
Published by the AIP Publishing

Strain-induced energy gap variation in ZnTe/ZnMgTe core/shell nanowires

P. Wojnar,[1,a)] M. Zielinski,[2] E. Janik,[1] W. Zaleszczyk,[1] T. Wojciechowski,[1] R. Wojnar,[3] M. Szymura,[1] Ł. Kłopotowski,[1] L. T. Baczewski,[1] A. Pietruchik,[1] M. Wiater,[1] S. Kret,[1] G. Karczewski,[1] T. Wojtowicz,[1] and J. Kossut[1]
[1]*Institute of Physics, Polish Academy of Sciences, Al Lotników 32/46, PL-02-668 Warsaw, Poland*
[2]*Institute of Physics, Faculty of Physics, Astronomy and Informatics, Nicolaus Copernicus University, ul Grudziądzka 5, PL-87-100 Toruń, Poland*
[3]*Institute of Fundamental Technological Research, Polish Academy of Sciences, Pawińskiego 5B, PL-02-106 Warsaw, Poland*

(Received 21 March 2014; accepted 14 April 2014; published online 25 April 2014)

Strain-induced changes of ZnTe energy gap in ZnTe/ZnMgTe core/shell nanowires arising from lattice mismatch between the core and the shell semiconductor are studied by means of optical methods. It is shown that the increase of the Mg content in the shell, as well as the increase of the shell thickness result in an effective redshift of the near band edge photoluminescence from ZnTe nanowire cores, which reflects directly the decrease of energy gap under tensile strain conditions. The conclusions are supported by theoretical calculations in terms of the valence force field model. The observed change of ZnTe energy gap can be as large as 120 meV with respect to the unstrained conditions and can be tuned in a continuous manner by adjusting shell parameters, which open a path towards an effective band gap engineering in these structures. © *2014 AIP Publishing LLC*. [http://dx.doi.org/10.1063/1.4873355]

Nanowires grown in the core/shell geometry attract a great interest because of possible applications as building blocks of several devices, such as solar cells,[1] high electron mobility transistors,[2] light emitting diodes,[3,4] and lasers.[5] The presence of coating shells improves considerably the optical and carrier transportation properties of nanowires due to passivation of surface states.[6,7] This issue is particularly important in nanowires due to a relatively large surface to volume ratio which is characteristic for these structures.

Strain originating from the lattice mismatch between the core and the shell material is an inherent property of core/shell nanowires. The value of the strain acting on a nanowire core can be controlled by shell parameters, such as the shell thickness and shell composition. For instance, it has been shown recently that increasing the shell thickness results in an effective increase of the strain acting on the core of the nanowires.[8,9] There is, however, only a limited number of papers which address the impact of the strain on the energy landscape in the core/shell nanowires.[7,10–12] These reports describe properties of nanowires built of III-V semiconductors. The impact of the strain in II-VI nanowire heterostructures remains relatively unexplored.[13] In a recent publication,[14] energy shifts of the excitonic emission from ZnTe nanowires under strain conditions are well reproduced by quantitative calculations, whereas two experimental points are considered: one for the compressive strain and one for tensile strain (based on the results of Ref. 17).

In the present work, the impact of strain on the energy gap of ZnTe nanowires embedded in ZnMgTe coating shells is studied in a systematic manner. We vary the shell thickness and the Mg concentration in the shell and find that both parameters can significantly influence the energy gap of ZnTe nanowire cores. Moreover, we show that the tensile strain is responsible for the observed effects. The maximum value of the energy gap shift is as large as 120 meV with respect to unstrained bulk ZnTe and can be tuned in a continuous way by changing the shell parameters.

ZnTe nanowires are grown on Si substrate by molecular beam epitaxy using gold catalysts assisted vapor-liquid-solid growth mechanism[15] at 410 °C. The preferential nanowire crystallographic growth direction is [111]. For the deposition of ZnMgTe shells, the substrate temperature is reduced down to 360 °C,[16,17] which results in freezing of the Au/Si eutectic alloy droplet and epitaxial growth in the radial direction of the nanowire. In Figures 1(a)–1(c), scanning electron microscope (SEM) images of nanowires with various shell thicknesses are shown. The deposition time of the shell ranges from 2 min up to 8 min. For each sample, statistical mean values of the nanowire diameters after measuring about 100 nanowires are determined and plotted vs. the deposition time of the shell, Figure 1(d). We observe a well pronounced increase of the average nanowire diameter with increasing deposition time of the shell, which enables to determine the average ZnMgTe shell thickness, right scale in Figure 1(d). The shell thickness ranges from 3 nm to 2 min deposition time reaching up to 14 nm for 8 min ZnMgTe deposition time. Mg concentration in the nanowire shell is determined by means of energy dispersive X-ray diffraction as a statistical average of several individual nanowires and varies from 13% up to 35% depending on the Mg-cell temperature during the growth. The variation of the Mg content in different samples is consistent with the variation of Mg fluxes during the growth.

Next, optical properties of nanowires are studied. First of all, it is confirmed that ZnTe/ZnMgTe core/shell nanowires emit light at energies close to the energy gap of ZnTe. Several individual nanowires are studied by means of

a)Author to whom correspondence should be addressed. Electronic mail: wojnar@ifpan.edu.pl.

cathodoluminescence (CL). Figure 2(a) represents a SEM image of an individual ZnTe/ZnMgTe core/shell nanowire with the shell thickness of about 10 nm and Mg content of 0.29. The corresponding CL signal from this nanowire is characterized by an emission at 2.31 eV, i.e., in the near band edge (NBE) emission region of ZnTe (inset in Figure 2(a)). The clear confirmation of the origin of this emission is obtained after performing monochromatic CL mapping at 2.31 ± 0.2 eV, Figure 2(b), where the shape of the nanowire is nearly perfectly reproduced.

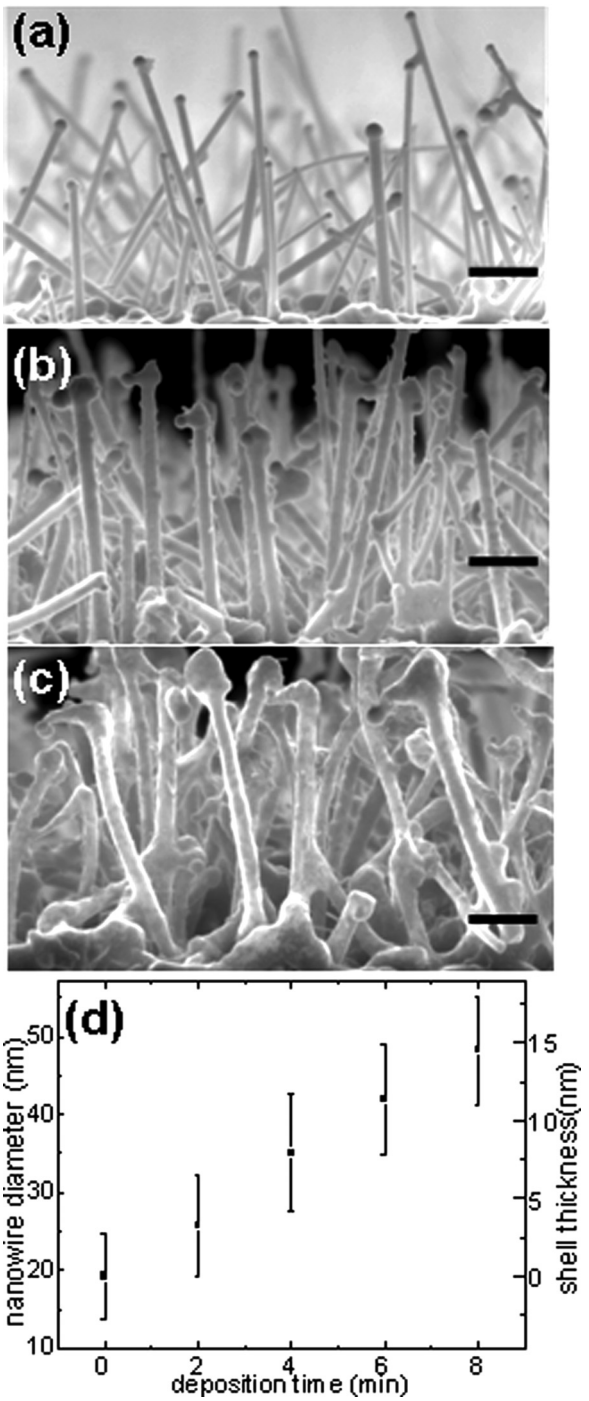

FIG. 1. ZnTe/ZnMgTe core/shell nanowires with various shell thicknesses (a) SEM images of uncapped ZnTe nanowires (b) and (c) nanowires with average ZnMgTe shell thickness of 8 nm and 14 nm, respectively, all scale bars are 200 nm. (d) Average nanowire diameter vs. ZnMgTe deposition time. Right scale: average shell thickness determined as the difference of the ZnTe/ZnMgTe and bare ZnTe nanowire diameters.

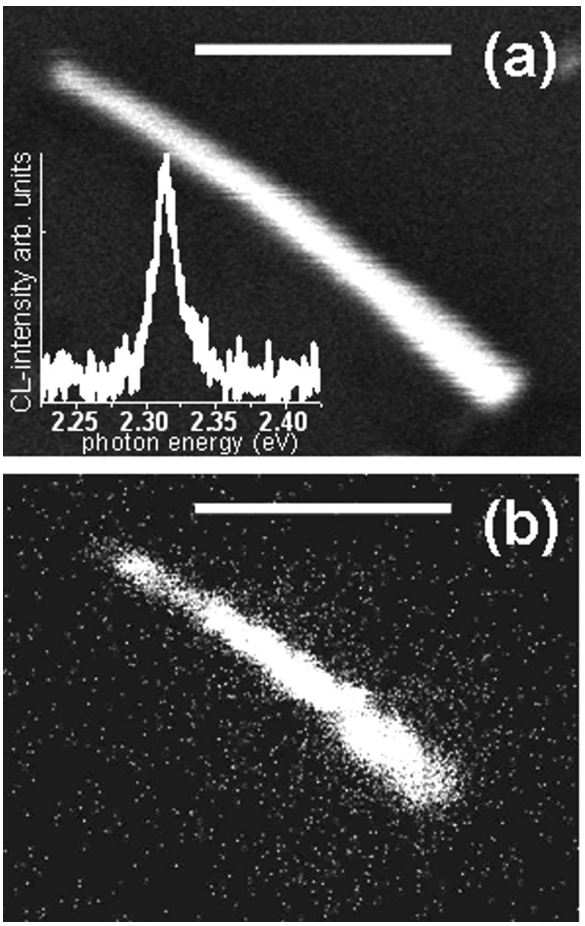

FIG. 2. Cathodoluminescence (CL) of an individual ZnTe/ZnMgTe core/shell nanowire, (a) SEM image of the nanowire with corresponding CL spectrum at 5 K in the inset, probe current 200 pA, scale bar 500 nm (b) monochromatic CL mapping at 2.31 ± 0.2 eV of the same spatial area.

The photoluminescence spectra at the energies corresponding to the ZnTe NBE emission region from ensembles of nanowires with various shell parameters are plotted in Figures 3(a) and 3(b). Results for nanowires with various average shell thicknesses ranging from 3 nm up to 14 nm and an almost constant Mg concentration of about 0.35 ± 0.03 are presented in Figure 3(a). A clear red shift of the emission with an increasing shell thickness is observed. A similar effect is observed in Figure 3(b) for samples with various Mg concentrations in the ZnMgTe shell and almost the same average shell thickness of about 14 ± 5 nm. A clear redshift of the NBE-emission with increasing Mg concentration in the shell is shown, whereas the maximum shift amounts to 120 meV with respect to the value of unstrained ZnTe, 2.380 eV. It is important to note that all emission lines in Figure 3 are normalized since with an increasing shell thickness and Mg concentration, the NBE emission intensity of ZnTe increases by orders of magnitude. The uncapped ZnTe nanowires do not exhibit any emission in the NBE emission region despite of excellent monocrystalline structure. In contrast, ZnTe nanowires grown at a different temperature and on a different substrate[14] exhibit some emission in this spectral region. This difference can be explained by the fact that the variation of the growth procedure may result in different effects on the surface of nanowires, such as, e.g., changes in the thickness of the oxide layer.

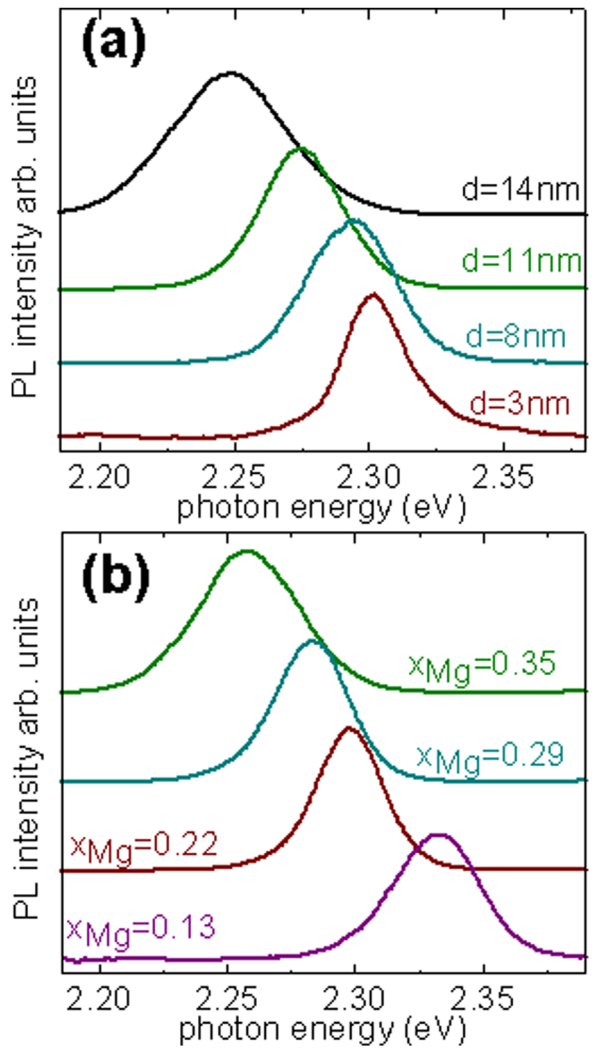

FIG. 3. Near band edge emission from ZnTe nanowire cores with various shell parameters: (a) impact of the ZnMgTe shell thickness 3, 8, 11, and 14 nm with a fixed Mg content at 0.35 (b) impact of Mg concentration on the emission energy and Mg content varying from 0.13 up to 0.35 with a fixed average shell thickness of 14 nm, T = 5 K, non-resonant excitation 405 nm.

Several effects may influence the NBE emission energy from nanostructures including strain, diffusion of atoms across heterointerfaces, and quantum size effect. It will be, subsequently, shown that the strain makes a predominant contribution in the case of ZnTe/ZnMgTe core/shell nanowires. A significant influence of the diffusion of Mg atoms across the core/shell interface can be excluded basing on the dependence of the emission energy on the Mg content in the shell presented in Figure 3(b). The increase of the Mg content should lead to an increase of the number of Mg atoms entering into the nanowire core and shift the emission energy toward higher energies. In contrast, the increase of the Mg content in the shell causes a clear decrease of the emission energy from nanowire cores, Figure 3(b). This finding contradicts to the predominant contribution of diffusion effects on the emission energy.

Another effect that may influence the emission energy from nanostructures is the quantum size effect. The increase of Mg content in the shell should increase the depth of the confining potential. As a result, one would expect an increase of the emission energy with increasing Mg content in the shell. As already mentioned, the opposite effect is observed in Figure 3(b). Moreover, the quantum size effect in studied structures is expected to be negligible, because of relatively large diameters of the nanowire cores, 19 ± 5 nm, as observed in SEM images, Figure 1(a). The negligible impact of the quantum size effect is confirmed by PL-measurements, where the emission energy of all lines presented in Figures 3(a) and 3(b) appears at energies lower than the free exciton energy of unstrained bulk ZnTe, 2.380 eV.

On the other hand, results presented in Figures 3(a) and 3(b) are consistent with the interpretation in terms of strain induced changes of the energy gap. The increase of Mg concentration in the shell increases the lattice mismatch between the core and shell semiconductor, resulting in the effective increase of tensile strain acting on the core of a nanowire. Similar effect is caused by the increase of the ZnMgTe shell thickness.[8,9] In the limit of thin shells, the lattice constant of the nanowire cores remains unchanged, whereas with increasing shell thickness it tends to reach the lattice parameter of the ZnMgTe shell increasing simultaneously the tensile strain.

It should be noted that when the shell thickness exceeds a critical value,[18–20] the strain may relax forming dislocations in the core and shell region. High optical quality of studied core/shell nanowires indicates, however, that this critical shell thickness is not reached in our structures.

Summarizing the above considerations, ZnTe/ZnMgTe core/shell nanowires represent a convenient system for decoupling the strain induced effects from the quantum size effect and diffusion effects. Whereas the tensile strain is expected to redshift the emission energy; and the quantum size effect and the Mg diffusion are expected to blueshift the emission energy. The spectral shifts presented in Figures 3(a) and 3(b) are qualitatively consistent with the interpretation in terms of strain induced changes of ZnTe energy gap.

The uniaxial anisotropy of nanowires implies several interesting properties of strain state in the presence of a lattice mismatched shell. In such situation, as already revealed by other authors,[12,18,21] the core of the nanowire is strained uniformly within the entire core region with the predominant strain contribution due to the axial strain. At this stage, it is important to clarify whether the observed values of the energy gap variation can be induced by the strain only, or other effects must be taken into consideration.

In order to obtain numerical values of expected energy gap decrease, theoretical calculations are performed. They involve two main steps: (a) calculation of equilibrium positions of constituent atoms and the resulting strain distribution, (b) calculation of the effective gap shift due to strain. In this work, we use an approach with the calculation of atomic positions (relaxation of strain) included via the atomistic valence force field (VFF) theory.[22–26] Nanowires are modeled as a cylindrical ZnTe core with the lattice constant of 6.103 Å surrounded by ZnMgTe shell with the lattice constant increasing linearly with the Mg content up to the value of 6.420 Å for pure MgTe.[27] The core diameter is equal to 19 nm. The nanowire length is equal to 250 nm. We have, however, checked that the results do not change significantly when increasing the nanowire length up to 500 nm and 1000 nm (the difference is less than 1 meV). The shell thickness is varied from

TABLE I. VFF parameters d, α, and β for ZnTe and MgTe. The bulk elastic constants c_{11}, c_{12}, c_{44}, and bulk modulus $K = (c_{11} + 2c_{12})/3$ are compared with experimental or theoretical data (in parentheses).[27–30]

	d (Å)	α (N/m)	β (N/m)	c_{11} (GPa)	c_{12} (GPa)	c_{44} (GPa)	K (GPa)
ZnTe	2.6427	29.1	5.71	75.8 (71.1)	38.3 (40.7)	31.3 (31.3)	50.83 (57.83)
MgTe	2.7799	25.2	6.45	69.4 (62.0)	29.2 (32.9)	32.0 (32.0)	42.6 (42.6)

1.2 nm (4 monolayers) up to 20 nm, with a 1.2 nm step giving total 15 values of different diameters. The Mg content in the shell area is varied from 6% to 42% with a 3% step, i.e., we consider 13 different shell compositions. This results in a family of total 195 different systems used for computations.

The computational domain for the strain calculation has reached over 10^7 atoms.[31] We assume free boundary conditions at the surface of the nanowire, whereas the overall size of the computational domain (in particular the nanowire length) guarantees convergence of the strain distribution at the center of the nanowire.[31,32] For ZnTe and MgTe, we developed new sets of VFF parameters,[26] see Table I. These parameters are obtained by a fit[33] aiming to reproduce bulk elastic constant c_{44} and bulk modulus $K = (c_{11} + 2c_{12})/3$. Such approach results in the VFF parameters optimized for the [111] nanowire growth.[24] Once the equilibrium atomic positions are known, we calculate resulting strains and finally the effective gap shift caused by strain. Due to relatively large core diameter, nanowire bands evolution under external strain ε can be modeled as that of nearly bulk-like ZnTe core. This corresponds to the assumption of limited core states decay into the shell and neglecting small (several meV) correction due to excitonic effects. Therefore, the effective nanowire band gap shift can be approximated as

$$E_{gap}^{NW}(d,\varepsilon) \approx E_{gap}^{ZnTe}(d \rightarrow bulk, \varepsilon = 0) + \Delta_{bulk}^{strain}(\varepsilon),$$

where $E_{gap}^{ZnTe} = 2.380\,\text{eV}$ is the ZnTe bulk band-gap at $T = 5\,K$ and $\Delta_{bulk}^{strain}(\varepsilon)$ describes bands evolution under strain ε.

We model $\Delta_{bulk}^{strain}(\varepsilon)$ using Bir-Pikus Hamiltonian,[34–36] where the conduction band shift is given in terms of the trace of the strain tensor and the bulk deformation potential, whereas for holes we explicitly solve (diagonalize) 6×6 strain Hamiltonian. For the calculation of nanowire bands evolution, we use strain values obtained at the center of the nanowire by the prior VFF calculation, whereas there are overall 3 empirical parameters used in the band gap shift calculation:[29] $a_g = a_c - a_v = 5.8\,\text{eV}$ band gap deformation potential, $b = -1.8\,\text{eV}$ biaxial [001], and $d = 4.61\,\text{eV}$ shear [111] strain deformation potentials.

It is found that there is a pronounced nanowire effective gap reduction with increasing Mg content in the shell and the shell thickness, e.g., for Mg content $x = 0.36$ and shell thickness 10 nm, there is 125 meV red-shift with respect to the uncapped ZnTe nanowire. For [111] grown systems, most of the gap evolution is due to hydrostatic tensile strain, contributing to about 75% of the total shift band gap via band gap deformation potential a_g, whereas [111] axial (shear) strains contribute to about 25% of the total shift through the shear strain deformation potential d. The contribution due to biaxial [001] strain (related to b deformation potential) is practically negligible. Beside the energy gap variation, the [111] shear strain leads to the light and heave hole splitting with the heavy holes being the ground state. The in-plane strain, perpendicular to the growth direction, is at least one order of magnitude smaller than the strain in the [111] growth direction.

In Figure 4, the experimentally observed ZnTe emission energy shifts are compared to the theoretical model describing the variation of the energy gap under tensile strain conditions. The experimental points are determined from the spectra presented in Figure 3, whereas vertical error bars reflect the spectral width of the emission lines. The horizontal error bars in Figure 4(a) reflect the statistical variation of the Mg concentration in the shell. The average shell thickness shown in Figure 4(b) is determined from the difference

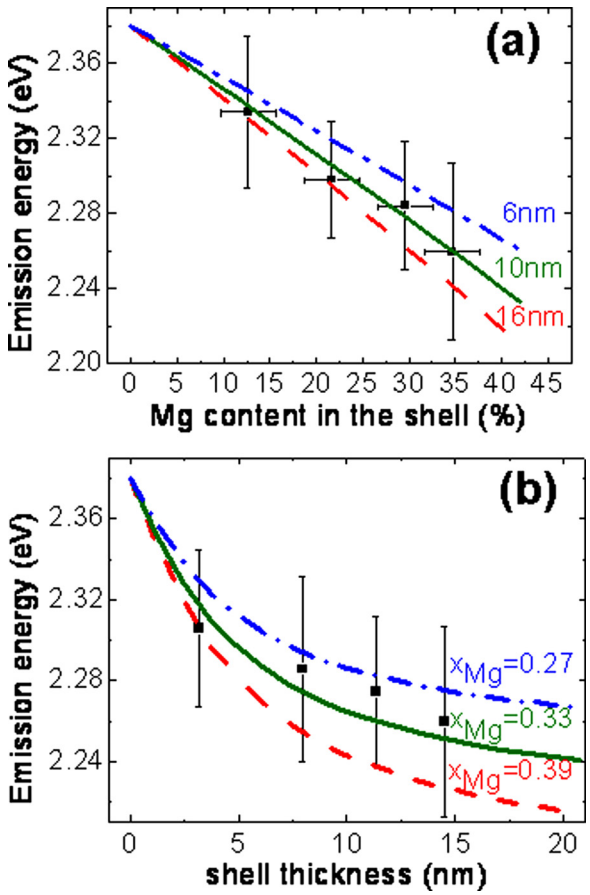

FIG. 4. Tensile strain induced energy shift from ZnTe nanowire cores, lines—theoretical model, points—experiment (a) dependence of the energy gap on the Mg content in the shell; shell thickness constant within the range 14 ± 5 nm, theoretical lines for shell thickness 6, 10, and 16 nm (b) dependence on the shell thickness; Mg concentration constant within the range 0.35 ± 0.03, theoretical lines for Mg content 0.27, 0.33, 0.39.

of the average diameter values of nanowires with and without ZnMgTe shells, shown above in Figure 1(d). Horizontal error bars related to the uncertainty of this quantity are not shown for clarity reasons, because they are relatively large and amount to about 7 nm. A satisfactory agreement between the experiment and theory is found. In particular, the observed large energy gap variation of the order of tens of meV is well reproduced by the theoretical calculations. Therefore, we conclude that the observed energy shifts are caused mostly by strain effects.

In conclusions, ZnTe/ZnMgTe core/shell nanowires with various shell parameters such as shell thickness and shell composition are grown by molecular beam epitaxy and studied by photoluminescence measurements. Depending on the shell parameters, the NBE emission from ZnTe nanowire cores exhibits significant spectral shift with the maximum value of 120 meV with respect to the emission energy of unstrained ZnTe. After excluding the main contribution of diffusion effects and quantum size effect to the emission energy, the observed spectral shift is attributed mainly to strain originating from the lattice mismatch between the core and shell semiconductor. This conclusion is supported by theoretical calculations in terms of VFF model which reproduces well the energy gap variation under tensile strain conditions.

This research has been supported by the European Union within European Regional Development Fund through Innovative Economy Grant (POIG.01.01.02-00-008/08), National Centre of Science (Poland) Grant DEC-2011/01/D/ST5/05039, and Ministry of Higher Education (Poland) Grant IP 2011061171. M.Z. acknowledges financial support from the Polish National Science Centre based on decision DEC-2011/01/D/ST3/03415.

[1]B. Tian, X. Zheng, T. J. Kempa, Y. Fang, N. Yu, G. Yu, J. Huang, and C. M. Lieber, Nature **449**, 885 (2007).
[2]X. Jiang, Q. Xiong, S. Nam, F. Qian, Y. Li, and C. M. Lieber, Nano Lett. **7**, 3214 (2007).
[3]F. Qian, Y. Li, S. Gradecak, D. Wang, C. J. Barrelet, and C. M. Lieber, Nano Lett. **4**, 1975 (2004).
[4]F. Qian, S. Gradecak, Y. Li, C. Y. Wen, and C. M. Lieber, Nano Lett. **5**, 2287 (2005).
[5]F. Qian, Y. Li, S. Gradecak, H. G. Park, Y. J. Dong, Y. Ding, Z. L. Wang, and C. M. Lieber, Nature Mater. **7**, 701 (2008).
[6]Y. Li, J. Xiang, F. Qian, S. GradeCak, Y. Wu, H. Yan, H. Yan, D. A. Blom, and C. M. Lieber, Nano Lett. **6**, 1468 (2006).
[7]N. Sköld, L. S. Karlsson, M. W. Larsson, M. E. Pistol, W. Selfert, J. Tragardh, and L. Samuelson, Nano Lett. **5**, 1943 (2005).
[8]A. Biermanns, T. Rieger, G. Bussone, U. Pietsch, D. Gruetzmacher, and M. I. Lepsa, Appl. Phys. Lett. **102**, 043109 (2013).
[9]K. Hestroffer, R. Mata, D. Camacho, C. Leclere, G. Tourbot, Y. Niquet, A. Cros, C. Bougerol, H. Renevier, and B. Daudin, Nanotechnology **21**, 415702 (2010).
[10]M. B. Bavinck, M. Zielinski, B. J. Witek, T. Zehender, E. P. Bakkers, and V. Zwiller, Nano Lett. **12**, 6206 (2012).
[11]M. Montazeri, M. Fickenscher, L. M. Smith, H. E. Jackson, J. Yarrison-Rice, J. H. Kang, Q. Gao, H. Tan, C. Jagadish, Y. Guo, J. Zou, M. E. Pistol, and C. E. Pryor, Nano Lett. **10**, 880 (2010).
[12]L. Rigutti, G. Jacopin, L. Largeau, E. Galopin, A. Bugallo, F. Julien, J. Harmand, F. Glas, and M. Tchernycheva, Phys. Rev. B **83**, 155320 (2011).
[13]E. Yoskovitz, G. Menagen, A. Sitt, E. Lachman, and U. Banin, Nano Lett. **10**, 3068 (2010).
[14]A. Artioli, P. Rueda-Fonseca, P. Stepanov, E. Bellet-Amalric, M. D. Hertog, C. Bougerol, Y. Genuist, F. Donatini, R. Andre, G. Nogues, K. Kheng, S. Tatarenko, D. Ferrand, and J. Cibert, Appl. Phys. Lett. **103**, 222106 (2013).
[15]E. Janik, J. Sadowski, P. Dluzewski, S. Kret, L. T. Baczewski, A. Petroutchik, E. Lusakowska, J. Wrobel, W. Zaleszczyk, G. Karczewski, T. Wojtowicz, and A. Presz, Appl. Phys. Lett. **89**, 133114 (2006).
[16]P. Wojnar, M. Szymura, W. Zaleszczyk, L. Klopotowski, E. Janik, M. Wiater, L. T. Baczewski, S. Kret, G. Karczewski, J. Kossut, and T. Wojtowicz, Nanotechnology **24**, 365201 (2013).
[17]P. Wojnar, E. Janik, L. T. Baczewski, S. Kret, E. Dynowska, T. Wojciechowski, J. Suffczynski, J. Papierska, P. Kossacki, G. Karczewski, J. Kossut, and T. Wojtowicz, Nano Lett. **12**, 3404 (2012).
[18]S. Raychaudhuri and E. T. Yu, J. Appl. Phys. **99**, 114308 (2006).
[19]C. Haapamaki, J. Baugh, and R. LaPierre, J. Appl. Phys. **112**, 124305 (2012).
[20]K. L. Kavanagh, J. Salfi, I. Savelyev, M. Blumin, and H. E. Ruda, Appl. Phys. Lett. **98**, 152103 (2011).
[21]T. E. Trammell, X. Zhang, Y. Li, L. Q. Chen, and E. C. Dickey, J. Cryst. Growth **310**, 3084 (2008).
[22]P. N. Keating, Phys. Rev. **145**, 637 (1966).
[23]R. M. Martin, Phys. Rev. B **1**, 4005 (1970).
[24]Y. M. Niquet, A. Lherbier, N. H. Quang, M. V. Fernandez-Serra, X. Blase, and C. Delerue, Phys. Rev. B **73**, 165319 (2006).
[25]M. Zielinski, Phys. Rev. B **86**, 115424 (2012).
[26]M. Zielinski, J. Phys.: Condens. Matter **25**, 465301 (2013).
[27]J. M. Hartmann, J. Cibert, F. Kany, H. Mariette, M. Charleux, P. Alleysson, R. Langer, and G. Feuillet, J. Appl. Phys. **80**, 6257 (1996).
[28]P. Bhardwaj, S. Singh, and N. K. Gaur, Turk. J. Phys. **32**, 85 (2008).
[29]H. Landolt and R. Bornstein, *Semiconductors, Physics of IV, III-V, II-VI and I-VII Compounds* (Springer, Berlin, 1982), Vol III/17 B.
[30]S. Mnasri, S. B.-B. Nasrallah, N. Sfina, N. Bouarissa, and M. Said, Semicond. Sci. Technol. **24**, 095008 (2009).
[31]M. Zielinski, Acta Phys. Pol., A **122**, 312 (2012).
[32]S. Lee, F. Oyafuso, P. von Allmen, and G. Klimeck, Phys. Rev. B **69**, 045316 (2004).
[33]There is a little unambiguous data available in the literature,[26,29] regarding MgTe bulk elastic constants, therefore, we use averaged value of $c_{44} = 32.0$ GPa. We found, however, that our results do not depend significantly on the choice of the VFF parameterization and the bulk elastic constants c44.
[34]G. L. Bir and G. E. Pikus, *Symmetry and Strain-Induced Effects in Semiconductors* (Wiley, New York, 1975).
[35]C. G. Van de Walle, Phys. Rev. B **39**, 1871 (1989).
[36]S. H. Wei and A. Zunger, Phys. Rev. B **49**, 14337 (1994).